Engineering Journal issn: 0125-8281

Article

Seismic Strengthening of RC Frame and Brick Infill Panel using Ferrocement and Expanded Metal

Suvawat Longthong[1,a], **Phaiboon Panyakapo**[1,b,*], **and Anat Ruangrassamee**[2]

1 Department of Civil Engineering and Town Development, School of Engineering, Sripatum University, Bangkok, Thailand
2 Department of Civil Engineering, Faculty of Engineering, Chulalongkorn University, Bangkok, Thailand
E-mail: [a]suvawatwin_53@hotmail.com, [b]phaiboon.pa@spu.ac.th (Corresponding author)

Abstract. This paper presents the strengthening of reinforced concrete frame and brick infill panel by using ferrocement technique reinforced with expanded metal. Analytical models of the strengthened frame and infill panel were proposed. An experimental study on the strengthened frames was conducted to verify the proposed models. Two control specimens and two strengthened specimens were compared: the bare frame and the infilled frame. Special strengthening techniques were employed to protect against two major failures: the beam and columns of the frame were fully strengthened to prevent shear failure, and the infill panel was protected against corner compression failure. The frames were investigated under constant vertical load and lateral cyclic load. The seismic behavior of the retrofit frames was compared with the control specimens. The strengthened frames showed the significant increase of strength up to 64% and 87%, and the ductility capacity was also improved 77% and 66% for the bare frame and the infilled frame, respectively. The proposed model of strengthening for the frame and infill panel predicted the lateral resistance of the RC infilled frame with a reasonable accuracy when compared to the observed experimental results.

Keywords: Seismic strengthening, reinforced concrete frame, infill panel, ferrocement, expanded metal.

ENGINEERING JOURNAL Volume 24 Issue 3
Received 31 October 2019
Accepted 6 March 2020
Published 31 May 2020
Online at https://engj.org/
DOI:10.4186/ej.2020.24.3.45

DOI:10.4186/ej.2020.24.3.45

1. Introduction

During 2014 Mae Lao earthquake which occurred in the northern part of Thailand, many existing reinforced concrete buildings were damaged under earthquake load. Among these, several school buildings which are typically reinforced concrete frame with brick infill panel were severely damaged owing to the brittle shear failure of the columns [1]. It is known that the effects of infill panel contribute significant strength to the frame [2]. These are characterized into three failure modes: diagonal compression, sliding shear and corner compression. Therefore, many techniques on the seismic strengthening of the infill frame have been conducted to retrofit the buildings. Among these, the use of ferrocement with expanded metal mesh reinforcement is an effective method to wrap the RC column. Kazemi and Morshed [3] investigated the efficiency of RC short columns strengthening with ferrocement jacket and expanded steel mesh. The strengthened specimens with various volume fraction of mesh reinforcement were tested under lateral cyclic loading. It was found that the shear strength and ductility capacity of the strengthened column were enhanced owing to the effect of confinement. In addition, the expanded steel mesh could decrease shear cracking. This is consistent with ACI 549.1R-93 [4] which reported that expanded metal mesh tends to minimize crack width, and it leads to desirable impact resistance and crack control.

One of the problems for the technique of mesh wrapping of ferroceemnt jacket is the effect of sharp curves, particularly for the case of rectangular column. Several researchers [5, 6] have proposed the jacketing with rounded corner column technique to improve the sharpness at the corners of rectangular column. Later on, the method was employed to improve the technique of ferrocement jacketing. Kaish et al. [7] investigated three jacketing techniques for square column. These included: the technique of square jacketing with rounded corner column, square jacketing with multi layers, square jacketing with shear keys. The specimens were tested under vertical concentric and eccentric loads. It was found that the first method which employed the rounded corner column showed the greatest load capacity for the eccentric load case. For the concentric load case, the triple layer mesh column provided the highest load capacity.

The strengthening technique of infill panel has been investigated by many researchers. Aykac et al. [8, 9] employed perforated steel plate to strengthen the infill wall steel frames. The perforated steel plates were fixed to the hollow brick wall by tightened bolts. Some additional reinforcement methods were applied at the wall corner: bolt densification, L-shape flat steel placement, and concrete block. The results of cyclic load test on the 12 strengthened specimens demonstrated that the specimens were very ductile with the drift ratio up to 10%. The increase of the lateral strength was between 1.3-2.3 times that of the reference specimen. Leeanansaksiri et al. [10] investigated the application of expanded metal for seismic retrofitting of masonry infill wall of the reinforced concrete frame. The brick infill panel was strengthened with ferrocement by laminating with the expanded metal lath and plastered with cement mortar. It was found that the strength of the strengthened specimen was superior to the control frame. However, the corner crushing of infill panel at the loading direction caused a shear failure of the column. It is recommended that special improvement is required to protect the failure at the wall corner. This finding is also consistent with the research discussed by Aykac et al. [11]. Ismail et al. [12] investigated the use of fiber reinforced cement mortar to strengthen reinforced concrete frames with masonry under cyclic load. The retrofit method employed various types of fiber grids and various shapes. Among these, the carbon strengthened samples showed the worst capacity comparing to basalt and glass, and the performance of basalt was the best. The lateral strength of fiber reinforced specimens was between 1.2 to 2.0 times that of the control specimen. Recently, Roudsari et al. [13] investigated the seismic behavior of a concrete frame retrofitted with steel plate. The strength of the strengthened specimen could be enhanced between 20% and 90% greater than the control frame. In addition, the stiffness of the retrofit frame was increased by 40% up to 230%. However, the results of perforated shear panel containing large difference in the area and the position of the holes could influence the results, further research study is required.

This study is the extended research on the use of ferrocement with expanded metal for strengthening the reinforced concrete infilled frame reported in the previous study [10]. Experimental study on reinforced concrete frames: the frame without wall and the frame with brick panel were conducted to improve the strengthening technique of the existing frames, particularly for the protection against corner crushing of infill panel that caused premature shear failure of column. Analytical modelling of the strengthened column and infill panel was proposed to predict the lateral strength of the infilled frame. The strengthened specimens were tested under lateral reverse loading with the control vertical load. The experimental results were compared with the control specimens as well as the analytical results obtained from the proposed models.

2. Model of Strengthened Infilled Frame

2.1. Analytical Modelling of Strengthened Frame

The model is composed of two main components: the strengthened frame and the strengthened infill panel. The strengthening technique of reinforced concrete frame is presented in Fig. 1a. To prevent the premature shear failure of the frame, the column is confined with ferrocement through the full height. For the beam, the length of ferrocement confinement is covered in the

plastic hinged region of the beam which is assumed as 1.5 time of the beam depth.

In the strengthening process of ferrocement, the steel angels are employed as the medium to connect the expanded metal mesh at each corner of the column. The steel angles are welded to the expanded metal mesh by welding electrode. The stress distribution due to the confinement is assumed to be uniformly distributed along each side of the column as shown in Fig. 1b. The plastic moment capacity of the strengthened column (M_{pc}) is considered as a combination of the plastic moment of the existing column (M_c) and the plastic moment of ferrocement (M_p^F) as follows:

$$M_{pc} = M_c + M_p^F \tag{1}$$

When the stresses of the steel angle and the expanded metal reach the plastic limit, the plastic moment of ferrocement may be calculated as the sum of the plastic moment of the steel angle and the expanded metal.

$$M_p^F = \sum_{i=1}^{n} \sigma_s \left(\frac{I_1}{C_1}\right)_i + \sum_{i=1}^{n} \sigma_{\exp} \left(\frac{I_2}{C_2}\right)_i \tag{2}$$

where σ_s and $\sigma_{\exp}$ are the stress at the plastic limit of the steel angle and the expanded metal, respectively; I_1 and C_1 are the moment of inertia and the distance from the centroid of column to the yield surface of the steel angle, respectively.

I_2 is the moment of inertia of the expanded metal, which can be computed as follows:

$$I_2 = 2\left\{\frac{bt_e^3}{12} + bt_e\bar{x}^2\right\} + 2\left\{\frac{t_e d^3}{12}\right\} \tag{3}$$

where *b, d, H* are the width, the depth and the height of the column, respectively; t_e is the effective thickness of the expanded metal; $\bar{x}$ is the distance from the centroid of column to the neutral axis of the expanded metal; C_2 is the distance between the centroid of the column and the expanded metal.

The lateral resistant of the strengthened bare frame (R_{BF}) can be calculated as follows:

$$R_{BF} = \frac{2(M_{pc} + M_{pj})}{H} = \frac{2\left(M_c + M_p^F + M_{pj}\right)}{H} \tag{4}$$

where M_{pj} is the smallest value of moment when compared among column, beam and joint.

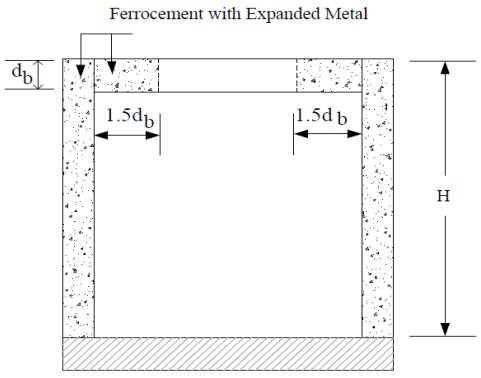

(a) RC Bare Frame

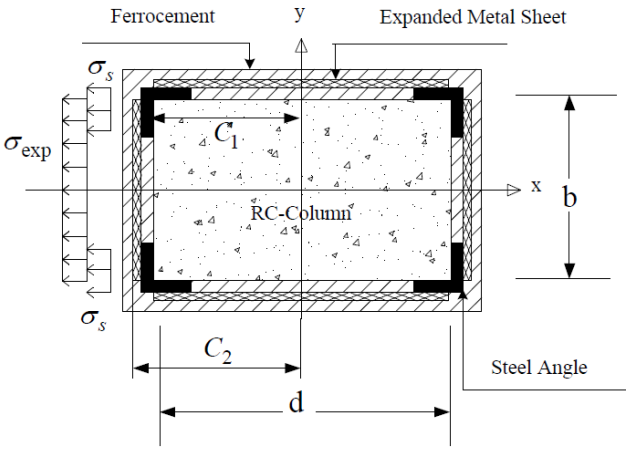

(b) Cross section of RC Column

Fig. 1. Strengthened bare frame.

2.2. Analytical Modelling of Strengthened Infill Panel

The infill panel is strengthened to enhance the strength for the three major failure mechanisms, i.e., diagonal compression, sliding shear, and corner compression failures. The model of strengthened infilled frame is shown in Fig. 2a, and the force envelope of diagonal strut for infill panel is shown in Fig. 2b. The strength of masonry panel for each failure mechanisms are calculated as the followings.

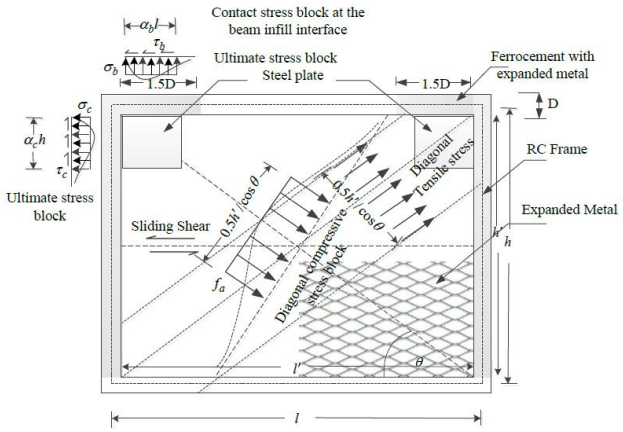

(a) Stress diagram of infill panel

DOI:10.4186/ej.2020.24.3.45

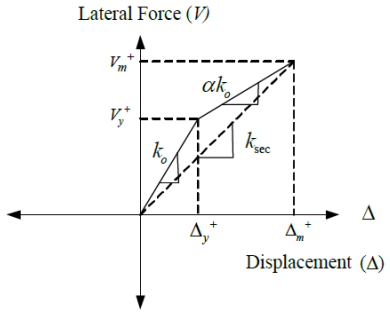

(b) Force envelope of diagonal strut

Fig. 2 Model of strengthening of RC frame and infilled panel.

2.2.1. Diagonal Compression Failure

The lateral yield strength V_y of the strengthened infill panel may be determined from the strength at cracking, which can be calculated based on the equation suggested by Saneinejad and Hobbs [14] as follows:

$$V_y = 2\sqrt{2}th' f_t \cos\theta \tag{5}$$

where $f_t = 0.25\phi\sqrt{f_m'}$ (MPa), $\phi = 0.65$, t, h' are the wall panel thickness (mm) and the wall panel height (mm) and f'_m is the masonry compressive strength (MPa) obtained from the strengthened masonry prism test.

To improve the compressive strength of the masonry panel, the strengthening technique is proposed by applying the ferrocement strengthened with expanded metal lath. The maximum strength V_m in the lateral direction is considered from the compressive stress block presented in Fig. 2a.

$$V_m = R_{DC}\cos\theta = 0.5h'tf_a \tag{6}$$

where $f_a = 0.6\phi f_m'$, $\phi = 0.65$.

In addition, the shear force that is carried by the diagonal tensile stress resulting from the strengthened expanded metal should improve the lateral strength of the wall panel. In this study, the lateral shear strength due to diagonal tension resistance is calculated as follows:

$$V_m = R_{DT}\cos\theta = \phi S_s A_n \cos\theta \tag{7}$$

where $\phi = 0.3$, S_s is the shear strength of the diagonal tension test of the strengthened masonry, A_n is the area of diagonal tensile stress, $A_n = (0.5h'/\cos\theta)\cdot t$.

2.2.2. Corner compression failure

For the resistance at the wall corner, the strength in the lateral direction of the wall panel V_m is a combination of compressive stress at column and shear stress at beam [14]:

$$V_m = R_{cc}\cos\theta = (1-\alpha_c)\alpha_c th\sigma_c + \alpha_b tl\tau_b \tag{8}$$

where

$$\alpha_c = \frac{1}{h}\sqrt{\frac{2M_{pj} + 2\beta_c M_{pc}}{\sigma_c t}} \tag{9}$$

$$\alpha_b = \frac{1}{l}\sqrt{\frac{2M_{pj} + 2\beta_b M_{pb}}{\sigma_b t}} \tag{10}$$

$$\sigma_c = \frac{f'_m}{\sqrt{1+3\mu^2 r^4}} \tag{11}$$

$$\sigma_b = \frac{f'_m}{\sqrt{1+3\mu^2}} \tag{12}$$

$$\tau_b = \mu\sigma_b \tag{13}$$

M_{pc}, M_{pb} are the column moment and beam moment at plastic, respectively; μ is the friction parameter between the wall and the frame, r is the height to width ratio of frame, β_c, β_b are the multiplying parameters of column and beam.

Since the corner compression failure is typically occur due to the stress concentration at the upper corner of the masonry panel which is governed by the compressive strength of the masonry. In this study, the corner compression resistance of the infill panel is improved by providing the additional rectangular steel plate at the upper corners of the infill panel as shown in Fig. 2a. The bearing resistance of the steel plate (R_{bs}) can be calculated as follows:

$$R_{bs} = t_p d_p f'_{mt} \tag{14}$$

where t_p, d_p are the thickness and the depth of the steel plate, respectively; f'_{mt} is the compressive strength of finishing mortar.

Therefore, the total resistance at the corner of the strengthened wall panel is the combination of Eq. (8) and Eq. (14).

$$V_m = (1-\alpha_c)\alpha_c th\sigma_c + \alpha_b tl\tau_b + t_p d_p f'_{mt} \tag{15}$$

2.2.3. Sliding Shear Failure

The sliding shear resistance of the infill panel is considered at the mid-height of the infill panel, which can be calculated by the following equation [14]:

$$R_{ss} = \frac{\gamma v t l'}{1 - 0.45 \tan\theta'} \quad (16)$$

where γ is the multiplying factor of the shear strength; v is the masonry shear strength. The parameter $\tan\theta'$ is computed by using the geometry of the infill panel.

$$\tan\theta' = (1 - \alpha_c) b' / l' \quad (17)$$

For the infill panel strengthened with expanded metal, the shear resistance may be calculated based on the suggestion of ACI549.1R-93 [4]:

$$V_s = \eta v_f A_v f_s \quad (18)$$

where V_s is the shear resistance of the ferrocement reinforced with expanded metal, η is the global efficiency factor of the mesh reinforcement, in this study, η=0.46 is employed for the expanded metal subjected to shear according to Panyamul et al. [15], v_f is the volume fraction of the mesh reinforcement, A_v is the gross cross sectional area of the mortar, f_s is the strength of the expanded metal mesh.

Therefore, the sliding shear resistance of the infill panel strengthened with ferrocement and expanded metal is the sum of the shear resistance of the infill panel (Eq. (16)) and that of the expanded metal mesh (Eq. (18)).

Finally, the maximum lateral resistance of the strengthened infilled frame is the sum of the resistant of the strengthened RC frames (R_{BF}) and the least lateral resistance of the above failure mechanisms of the infill panel which is governed the design.

To determine the force envelope of diagonal strut as shown in Fig. 2b, the yield displacement Δ_y and the maximum displacement Δ_m of strengthened infill panel can be calculated by using the strain of the strengthened masonry prism test as follows:

$$\Delta_y = \varepsilon_y L_d / \cos\theta \quad (19)$$

$$\Delta_m = \varepsilon_m L_d / \cos\theta \quad (20)$$

where ε_y, ε_m are the yield strain and the maximum strain of the strengthened masonry prism, L_d is equal to the length of the strut across the wall:

$$L_d = \sqrt{(1 - \alpha_c)^2 h'^2 + l'^2} \quad (21)$$

The initial stiffness including the post-yield stiffness and the bilinear factor can be calculated:

$$k_o = V_y / \Delta_y \quad (22)$$

$$k_{sec} = V_m / \Delta_m \quad (23)$$

$$\alpha k_o = (V_m - V_y) / (\Delta_m - \Delta_y) \quad (24)$$

3. Experimental Investigation

3.1. Materials Properties

The reinforced concrete frame specimens were prepared for testing in the laboratory. The concrete mix of all specimens was designed for a cylindrical compressive strength of 21 Mpa at 28 days. The cement mortar for brick bedding was prepared with the volumetric proportion of cement to sand ratio of 1:4, and water to cement ratio of 0.45. For the plastered mortar of ferrocement, the mixture of 1:2 cement/sand and 0.45 w/c were employed. The 28 days compressive strength of the bedded mortar and the plastered mortar specimens were 7.22 and 22.25 Mpa, respectively according to ASTM C349-97 [16].

The longitudinal steel bars of 15 mm and 19 mm diameters were employed as the reinforcement of the beam and column. The transverse steel bar of 6 mm diameter was the stirrup reinforcement. The steel bars are SR24 grade conformed to TIS 20-2543 [17] with yield strength of 240 Mpa and the ultimate strength of 385 Mpa.

The expanded steel mesh employed in this study was the standard type with an overlapped diamond shape mesh pattern. The typical shape (Fig. 3) and the basic physical properties of expanded metal sheet (Table 1) are conformed to JIS G3351 [18] Standard. The steel mesh has the tensile strength 340 Mpa and 400 Mpa corresponding to the yield and the ultimate, respectively [19].

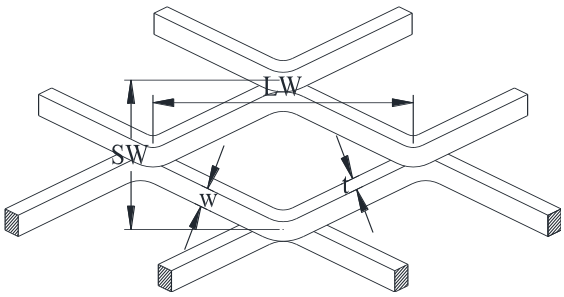

Fig. 3. Detail of expanded metal.

Table 1. Physical properties of expanded metal.

Type	SW (mm)	LW (mm)	t (mm)	w (mm)	Weight (kg/m^2)
Type 1	8.6	20	0.6	0.6	0.69
Type 2	34	76.2	4.5	4.5	9.68

In this study, the expanded metal lath type 1 was employed to strengthen the masonry panel which was based on the experimental results of the previous study

[10]. The result of the compressive strength of masonry prisms strengthened with the expanded metal lath type 1, which was conducted according to ASTM C1314-07 [20], was 9.07 Mpa. The result of the shear strength of the brick panels strengthened with the expanded metal lath type 1, which was performed according to ASTM E519-02 [21], was 2.60 Mpa. To strengthen the column and beam, the expanded metal type 2 was employed because the high percentage of reinforcement was required to enhance the shear strength of column and beam.

3.2. Test Specimens

The prototype reinforced concrete frame was chosen from the typical ground floor bay of a standard school building. The building was designed primarily for gravity load according to EIT 1007-34 [22] for non-seismic regions. The compressive strength of concrete and tensile strength of steel are 21 MPa and 240 MPa, respectively. The reinforcing details of the prototype frame are shown in Fig. 4a and Table 2. The transverse reinforcement of column has the gross sectional area of 169 mm^2 which was lower than the seismic requirement (490 mm^2) of the intermediate moment resisting frame. The stirrup of beam has a spacing of 200 mm which was also greater than the spacing limit of 175 mm. This indicated that the column and beam were designed with shear deficiency which may cause premature shear failure.

Table 2. Reinforcing details of the frame.

Member	Longitudinal		Transverse	
	Size (mm)	Area (mm^2)	Size (mm)	Area (mm^2)
Column	8RB19	2268	2RB6@200	169
Beam	5RB15	884	RB6@200	85

To prepare seismic strengthening of the existing reinforced concrete frames, the bare-frame BF and the infilled frame with brick panel IF was employed as the control specimens. For the retrofit specimens, the strengthened bare-frame BF-SR and the strengthened infilled frame with brick panel IF-SR were reinforced with ferrocement and expanded metal. The BF, BF-SR, IF, IF-SR specimens are presented in Fig. 4a-4d, respectively.

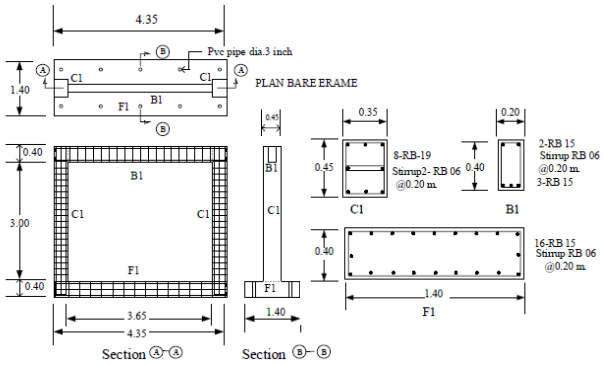

(a) Bare-Frame (BF)

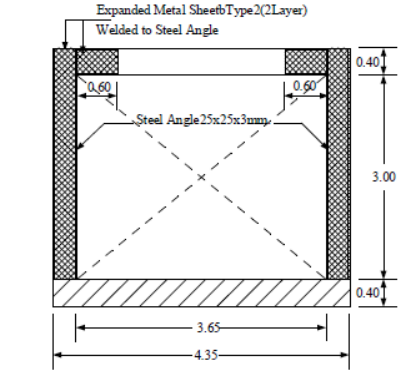

(b) Strengthened Bare Frame (BF-SR)

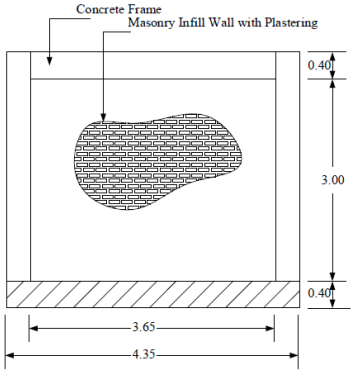

(c) Infilled Frame (IF)

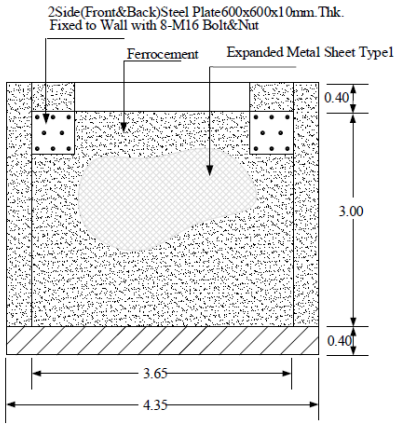

(d) Strengthened Infilled Frame (IF-SR)

Fig. 4. Selected reinforced concrete frames.

3.3. Strengthening Technique

In the strengthening process of BF-SR, four 25×25×3 mm steel angles were placed at each corner of columns and beams. The frame was confined by two layers of the expanded metal type 2 which was welded to the steel angle. The expanded metal mesh was fixed with 9 mm diameter steel tie rods that penetrated to the column at an embedded depth of 50 mm and a spacing of 150 mm along the height of columns. The tie rods were round bars with the yield strength of 240 MPa. They were grouted with the non-shrink cement as adhesive shear keys. The expanded metal was plastered with 30 mm thickness cement mortar. Details of the strengthening technique of the bare frame are shown in Fig. 5.

(a) Strengthened bare frame with expanded metal

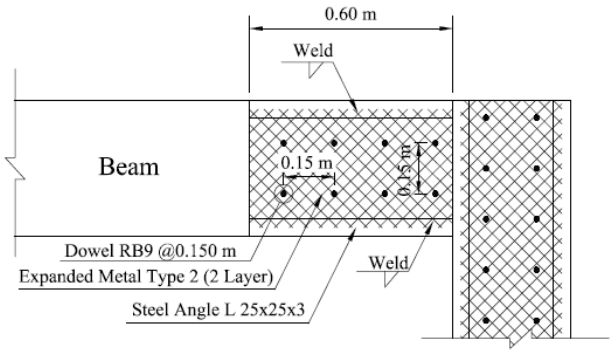

(b) Detail of strengthened beam

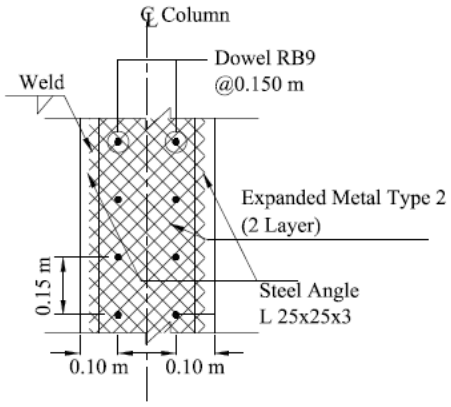

(c) Detail of strengthened column

Fig. 5. Details of strengthened bare frame (BF-SR).

For the strengthening process of the infilled frame IF-SR, the column and beam were strengthened with the same process as described for BF-SR. The infill panel was laminated both sides through the whole panel with the expanded metal type 1. The 6 mm bolts were employed to fix the expanded metal mesh with the brick panel at the spacing of 1.00 m. The expanded metal mesh was connected at the interface of brick panel and column by the 6 mm bolts at 300 mm spacing. The 600×600×10 mm steel plates were installed at both sides of the upper corners of infill panel. These steel plates were fixed to the wall panel with 8-M16 bolts that penetrated through the wall panel and tightened with the nuts. The penetrated holes of bolts were grouted with non-shrink cement to prevent the lateral movement of bolts. Finally, the infill panel was plastered by the cement mortar with the thickness equal to that of the steel plates. The use of rectangular steel plates was to improve the corner compression resistance of the infill panel. Details of strengthening infilled frame (IF-SR) are shown in Fig. 6.

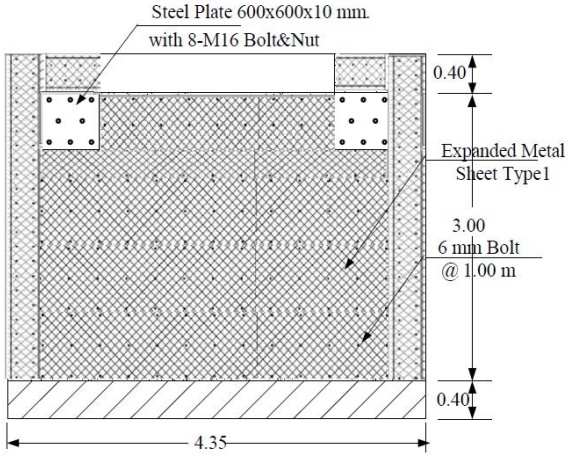

(a) Strengthening Infilled frame

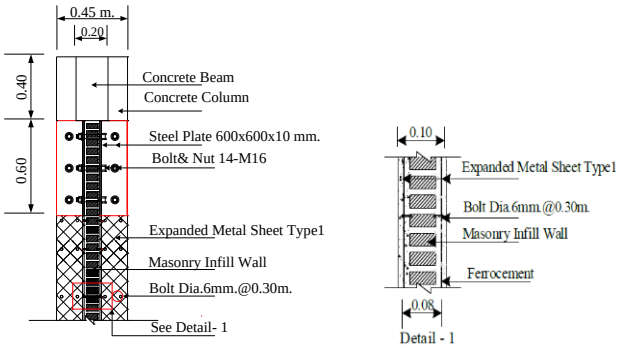

(b) Cross section at the corner of infill frame and enlarged detail of strengthened infill panel

Fig. 6. Details of strengthening infilled frame (IF-SR).

3.4. Test Devices and Loading System

The test setup of the retrofit brick panel frame with expanded metal (IF-SR) is presented in Fig. 7a. The foundation was fixed on the strong floor with five pairs

of anchored bolts. The columns were connected to the vertical hydraulic jacks for applying the 300 kN load. The frame was subjected to lateral cyclic load through a MTS 1500 kN hydraulic actuator. When the lateral load applied to push the specimen in one direction, the frame was drawn back in the opposite direction by a couple of 32 mm steel rod. The horizontal displacement of the specimen was recorded through the displacement transducers at the level of the applied lateral force. The curvatures at the base of both columns were measured through a set of displacement instruments installed at both sides of column. The loading protocol was performed according to FEM461 [23] by increasing the drift level with an increment of 0.1% until 0.5%. Then, the drift increment was changed to 0.25% until the strength of the specimen was decreased greater than 20% of the ultimate load. The loading protocol is shown in Fig. 7b.

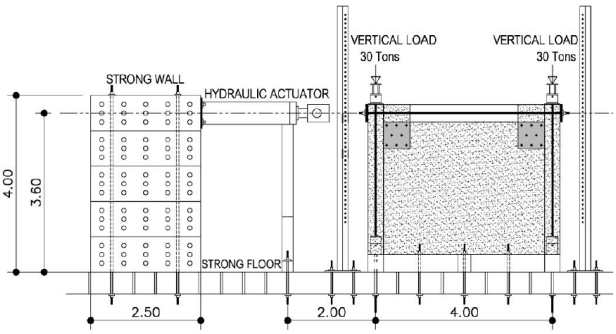

(a) Test setup of the experimental specimen IF-SR

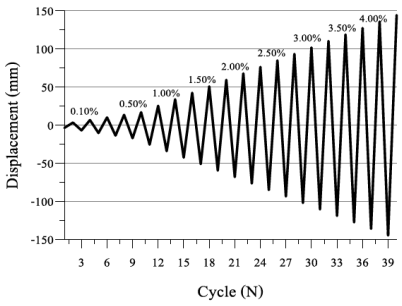

(b) Loading protocol

Fig. 7. Test setup and loading protocol of the experimental specimen

4. Experimental Results

4.1. Failure of the Specimens

For the control bare frame (BF) specimen, during the 0.5-1.0% drift, the crack occurred at the junction of beam and column connection due to the flexural failure. Further loading stage, 1.0-1.5% drift, slightly crack due to shear failure could be detected at both sides of the beam ends. When the frame sustained the lateral load to 2.0 % drift as shown in Fig. 8a, damage could be observed at the connection of column and beam where the crack appeared at the bottom of the column and beam connection as shown in Fig. 8b. The lateral load capacity of the bare frame is limited by the damage of beam rather than columns.

(a) 2% drift

(b) Crack at the beam-column joint

Fig. 8. Failure of the bare frame BF.

For the control infilled frame (IF) specimen, the diagonal crack of wall panel started at drift level 0.5% and followed by the slightly crack along the mortar bed joint at the mid height of the wall panel. The diagonal crack was enlarged when the drift level increased due to the increase of compressive stress in the diagonal direction. Meanwhile, the horizontal crack propagated further parallel to the concrete lintel level due to the excessive sliding shear. Furthermore, a slightly crack was observed at the wall corner near the actuator because the applied lateral load exerted high compressive stress through the wall. When the drift reached 1.5%, the infilled frame was failed due to the enlargement of diagonal crack and the sliding shear crack parallel to the mortar bed as shown in Fig. 9.

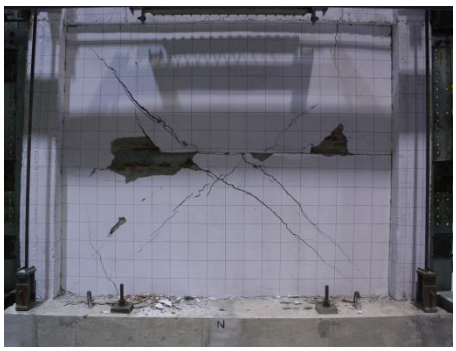

Fig. 9. Failure of the infilled frame IF (1.5% drift).

For the strengthened specimen BF-SR, when the test reached 1.0% drift, there were a few small cracks at the outer edge of the column base due to the increase of the flexural stress. When the frame continued to 2.0% drift, the crack started at the bottom of the beam-column joint. The specimen could carry the lateral load until it reached 4.5% drift as shown in Fig. 10a. The crack appeared at the connection of column and beam (Fig. 10b); however, they did not propagate any further. The cracks at the column base were enlarged (Fig. 10c), but there was no any significant crack. It was observed that the specimen BF-SR could sustain the lateral load up to the drift level 4.5% which is significantly larger than the control frame BF. In addition, the retrofit frame still maintained its stability at a satisfactory appearance which

indicated that the shear strength and the flexural strength of the beam-column components were significantly improved.

(a) 4.5% drift

(b) Failure at the beam

(c) Crack at the column base

Fig. 10. Failure mechanisms of BF-SR.

The crack patterns of the retrofit frame IF-SR corresponding to 0.50%, 0.75%, 1.00%, 1.25% drift are presented in Fig. 11a, 11b, 11c, 11d, respectively. During the initial loading 0.5% drift, the specimen was able to sustain the lateral load without any failure on the infill panel surface and the structural members. The first crack could be detected when the second test stage conducted up to 0.75% drift. The slightly crack started at the upper wall corner of the push loading direction due to the compressive stress in the diagonal direction. The diagonal crack propagated from the upper corner steel plate down to the base of infill panel. The crack width was gradually enlarged when the drift continued up to 1.25%. At the final test stage, an X-shaped crack pattern occurred at the middle region of infill panel as a result of the diagonal compression failure during the reverse cyclic loading as shown in Fig.11e. In addition, the corner compression failure of the mortar along the edge of the upper corner steel plate was found because the high compressive stress exerted at the push loading direction as shown in Fig. 11f. However, none of any crack caused by sliding observed on the infill panel. The beam and column still maintain load capacity without any shear failure.

(a) 0.50% drift

(b) 0.75% drift

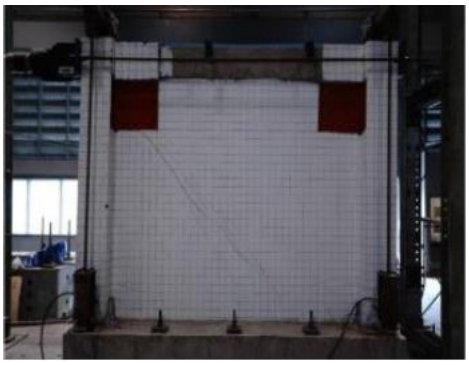

(c) 1.0% drift

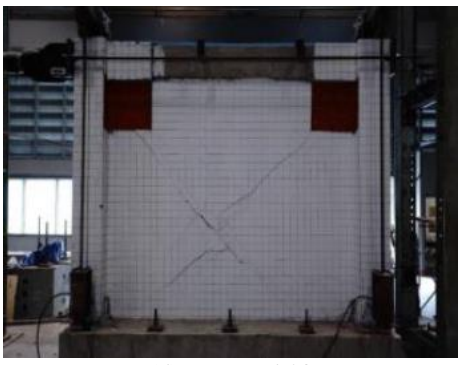

(d) 1.25% drift

(e) diagonal failure

(f) corner failure

Fig. 11. Failure of the strengthened specimen IF-SR.

DOI:10.4186/ej.2020.24.3.45

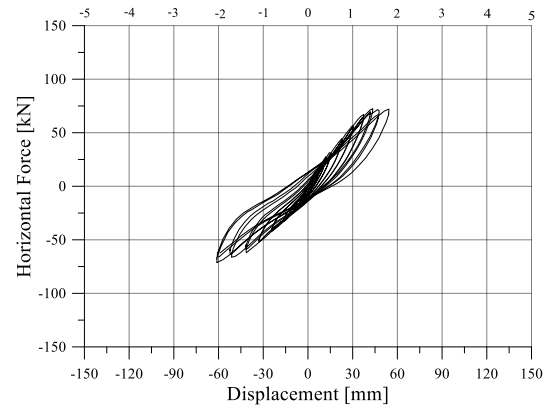

(a) BF

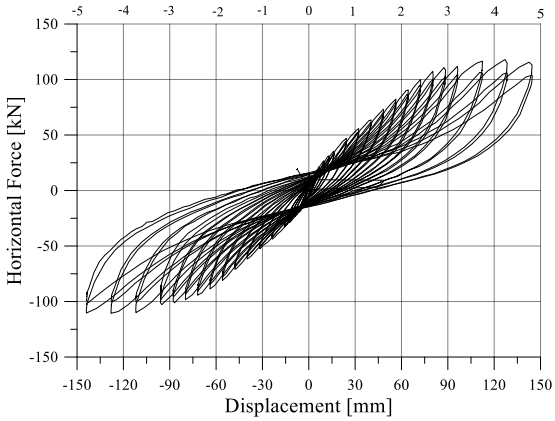

(b) BF-SR

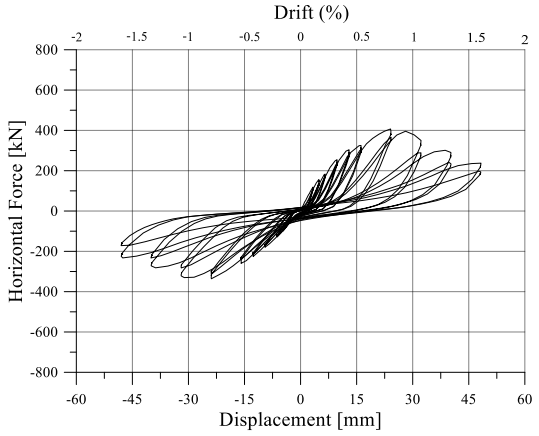

(c) IF

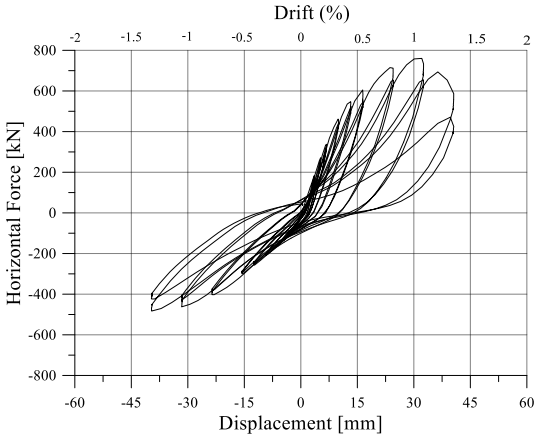

(d) IF-SR

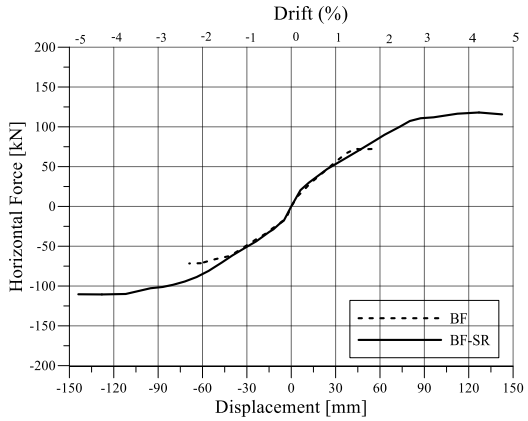

(e) Enveloped curves of BF and BF-SR

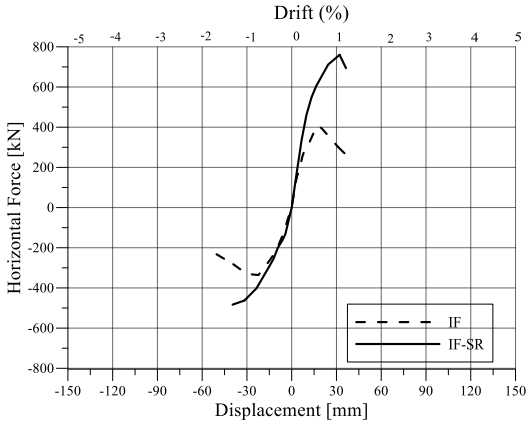

(f) Enveloped curves of IF and IF-SR

Fig. 12. Hysteretic behaviors of the specimens.

4.2. Hysteretic Behavior

The hysteretic behavior of the strengthened specimen is compared with those of the control specimens. The bare frame BF is compared with the strengthened bare frame BF-SR, as shown in Fig. 12a and 12b, respectively. The brick infilled frame IF is compared with the strengthened brick infilled frame IF-SR, as shown in Fig. 12c and 12d, respectively. The enveloped curves of the hysteresis behavior for these specimens are also presented in Fig. 12e-12f.

For the bare frame specimen BF, the frame maintained elastic during the applied load to 1.0% drift. Thereafter, the frame gradually degraded. The specimen retained the lateral load when the drift continued to 1.75% drift. The control bare frame BF showed thin hysteresis loop with the peak load of 72 kN. For the strengthened specimens BF-SR, the behavior remained elastic during the initial loading to 1.25% drift which was corresponding to the yield strength of 75 kN. After that drift level, the system exhibited inelastic behavior. The frame continued to retain the lateral strength during the increase of displacement until 4.19% drift, at which, the ultimate lateral strength was about 118 kN. The test was terminated because the system reached the target drift and there was no further increase of strength. The strengthening bare frame BF-SR exhibited much larger

hysteresis loop than that of BF, and it carried the greater load capacity with stable hysteresis loop shape. It is clear that the effect of strengthening enhanced the stiffness and strength of the bare frame.

The control brick infilled frame IF provided large hysteresis loops with the peak load of 407 kN owing to the effect of brick infill panel that increased the strength. However, the stiffness degraded significantly during the reloading because of the pinching behavior effect. For the retrofit frame IF-SR, the specimen behaved linear elastic up to 0.5% drift without any observed failure as mentioned above. The strength was developed up to 0.75% drift at which the first diagonal crack was observed, and thereafter the system started nonlinear behavior. When the system reached the peak load of 760 kN at 1.07% drift, severe cracking of the wall panel in the diagonal direction caused gradually loss of the resistance. This indicated that diagonal compression of the infill panel dominated the strength of the specimen. The test was terminated as the resistance was reduced to lower than 80% of the peak load. It was observed that the hysteresis response behaved un-symmetrical shape due to the lengthening of the steel rod during the reloading of the frame. However, the hysteresis loop of the strengthened frame IF-SR was significantly larger than the behavior of the frame IF. It was noticed from the enveloped curves of both specimens that the strengthened infill frame showed much greater strength and stiffness than that of the control specimen. It is obvious that the effect of the strengthened ferrocement with expanded metal significantly improved the stiffness and strength of the brick infilled frame.

4.3. Lateral Strength

The lateral strength at the yield point was defined by considering the intersection point of the initial stiffness and the post yield stiffness of the bilinear representation of the enveloped curve based on the method adopted by Panyakapo [24]. The strength and displacement at the yield level of the four specimens are shown in Table 3. The lateral load capacities of the specimens were calculated based on the capacity of control frame. Similarly, the strength, displacement, load capacity and displacement ductility at the maximum level of the four specimens are shown in Table 4. It is evident that the load capacities at the yield level of the strengthened frames BF-SR and IF-SR are 53% and 26% greater than those of the control specimens BF and IF, respectively. For the maximum level, the load capacities of the strengthened specimens BF-SR and IF-SR are 64% and 87% greater than that of BF and IF, respectively. The values of displacement ductility of the strengthened specimens BF-SR and IF-SR are also improved up to 77% and 66% when compared to the control specimens BF and IF, respectively. For the strengthened infill frame IF-SR, the increase of strength and ductility was due to the contribution of the confinement of frame and infill panel strengthened with ferrocement and expanded metal.

Table 3. Yield strength (V_y) and yield displacement (Δy) of the specimens.

Specimens	Drift %	V_y (kN)	Δ_y (mm)	Load Capacity
BF	0.67	49	20.00	1.00
BF-SR	1.25	75	37.50	1.53
IF	0.23	250	7.00	1.00
IF-SR	0.23	315	6.75	1.26

Table 4. Maximum strength (V_m) and ductility of the specimens.

Specimens	Drift %	V_m (kN)	Δ_m (mm)	Load Capacity	Ductility
BF	1.45	72	43	1.00	2.15
BF-SR	4.19	118	143	1.64	3.81
IF	0.67	407	20	1.00	2.85
IF-SR	1.07	760	32	1.87	4.74

4.4. Lateral Stiffness

The secant stiffness degradations of the four experimental samples are presented in Fig. 13. The stiffness degradation of the bare frame BF and BF-SR is relatively flat because the resistance of the frame was due to the flexural strength of beam and column without the contribution of infill panel. On the other hand, the stiffness of the infill frame specimens IF is greater than the bare frame BF due to the infill panel contribution. It is obvious that the strengthened infill frame specimen IF-SR provided the greatest stiffness due to the combined effect of the strengthened infill panel and the strengthened frame.

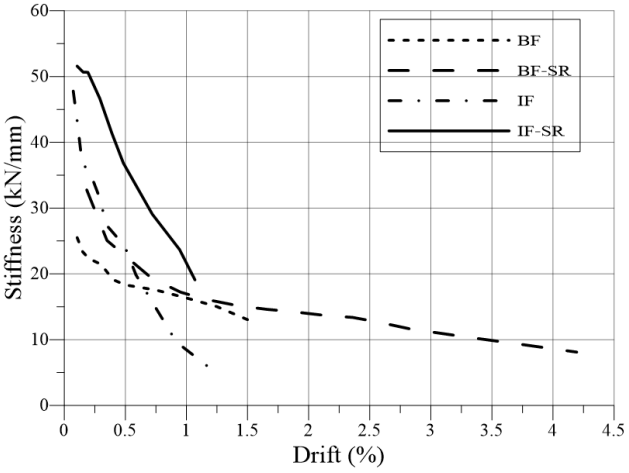

Fig. 13. Stiffness degradations of the four experimental samples BF, BF-SR, IF and IF-SR.

4.5. Energy Dissipation

The energy dissipation of the four specimens was calculated as the area enclosed by the hysteresis loops. The cumulative energy dissipation was plotted against the drift level as shown in Fig. 14. The specimens BF, BF-SR, IF and IF-SR provided the maximum cumulative energy dissipation 2500, 23700, 22500, 38200 kN-mm, respectively. It is clear that the strengthened specimen IF-SR dissipated the greatest amount of energy which is 15.28, 1.61, 1.70 times when compared to the BF, BF-SR, IF, respectively. This is the result of the strengthening infill panel as well as the retrofitted frame.

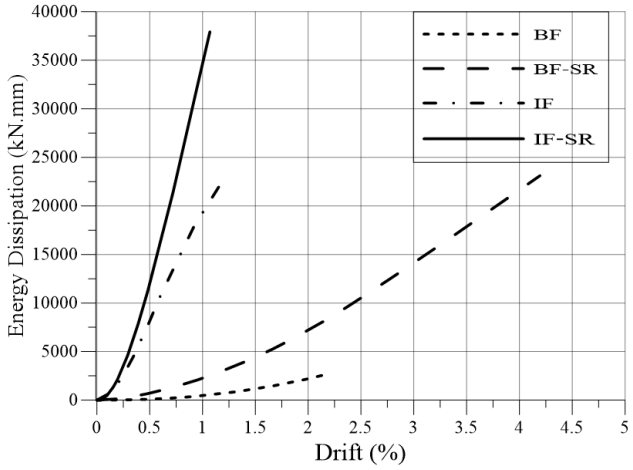

Fig. 14. Energy dissipation of the specimens BF, BF-SR, IF and IF-SR.

4.6. Verification of Analytical Modelling of Infill Panels

To verify the proposed analytical model that is described in the previous section, a simulation study of the proposed model was conducted by employing the computer program RUAUMOKO [25]. The reinforced concrete frame was modelled as a moment resisting frame. The moment capacity of the strengthened beam-column was calculated based on the proposed model. SINA degrading model [26] was determined as the flexure–shear hysteretic behavior of the column element as well as the beam. The infill panel was modelled as the equivalent strut by using nonlinear spring type member with Wayne Stewart degrading stiffness hysteresis [27]. The selection of this model is to allow the pinching behavior of infill panel observed in the experiment. To determine the force envelope of the equivalent strut for the infill panel, the hysteretic model parameters described in the previous section were calculated (Table 5). The compressive strength of the strengthened masonry prism, which is related to the infill panel strength, was taken from the masonry prism tests [10]. The comparison between the simulation results of bare frame and the experimental result is presented in Fig. 15a, similarly for the strengthened bare frame (Fig. 15b). The simulation results of infill panel and strengthened infill panel are shown in Fig. 16a and Fig. 16b, respectively. Finally, the simulation results of the frame with wall panel (IF) and the retrofit frame (IF-SR) are observed with the laboratory test results, as presented in Fig. 17a and Fig. 17b, respectively.

It can be observed that the stiffness (82.76 kN/mm) and strength (611.33 kN) of the strengthened infill panel are 57% and 93% greater than those of the ordinary infill panel (52.60 kN/mm and 316.28 kN) due to the effect of strengthening ferrocement together with expanded metal. The hysteresis loop shape of the strengthened infill panel is much larger than that of the ordinary infill panel, and hence, the more hysteretic energy dissipation. This leads to the greatest energy dissipation of the strengthened infill frame (IF-SR) which has been presented in the previous section. The analysis results reveal that the strength of infill panel has an important effect on the infilled frames. The strengths of infill panels (316.28 kN for IF and 611.33 kN for IF-SR) are 4.56 times and 5.53 times that of the bare frame BF (69.34 kN) and BF-SR (110.63 kN), respectively. The strength contribution of infill panel provided up to 82% and 85% of the overall infilled frames IF and IF-SR, respectively. The summary of the analysis results of infilled frame and strengthened infilled frame are compared with the experimental results as shown in Table 6. It was found that the analysis results of the overall strength of infilled frames IF and IF-SR are relatively close to the experimental results with 5.25% and 5.01% difference, respectively. The simulation results show that the characteristics of the hysteresis loop of the strengthened infill frame including the initial stiffness, the ultimate strength, and the pinching behavior are close to those of the laboratory test results. This demonstrates that the analytical model of the strengthening frame and infill panel can predict the lateral strength of the retrofit frame with a reasonable accuracy.

5. Conclusions

The analytical model of the brick infilled frame strengthened with ferrocement and expanded metal was proposed to predict the lateral strength of the retrofit frame. The proposed model was verified based on the experimental test and the simulation study of the strengthened specimens. The conclusions can be drawn as follows:

a) The lateral strength of the strengthened brick infill frame exhibited significant enhancement of strength that was greater than the control infill frame. This is primarily due to the diagonal compressive strength of the infill panel. It is evident from the experimental result that the technique of protection against the corner compression failure with the extra steel plates including the strengthening technique of the bare frame with ferrocement and expanded metal could successfully prevent the shear failure of columns.

b) The stiffness, strength and ductility of the strengthened brick infill frame were improved when compared to the control infill frame. The strengthened

specimens BF-SR and IF-SR are 64% and 87% greater than that of BF and IF, respectively. The values of displacement ductility of the strengthened specimens BF-SR and IF-SR are also improved up to 77% and 66%. The increase of stiffness and strength was due to the effect of the strengthened infill panel with ferrocement and expanded metal which provided up to 57% and 93% greater than those of the ordinary infill panel. The high contribution of the strengthened infill panel is due to the enhanced diagonal compressive strength of infill panel.

c) The strength of infill panel has an important effect on the infilled frames. The strengths of infill panels are 4.56 times and 5.53 times that of the ordinary bare frame (BF) and the strengthened bare frame (BF-SR), respectively. The strength contribution of infill panel provided up to 82% and 85% of the infilled frames (IF) and the strengthened infill frame (IF-SR), respectively. The simulation resulting from the analytical model for the strengthened infill frame is close to the experimental result with 5.01% difference. Therefore, the proposed model for the strengthened infill frame using ferrocement with expanded metal anticipated the lateral strength with a satisfactory accuracy.

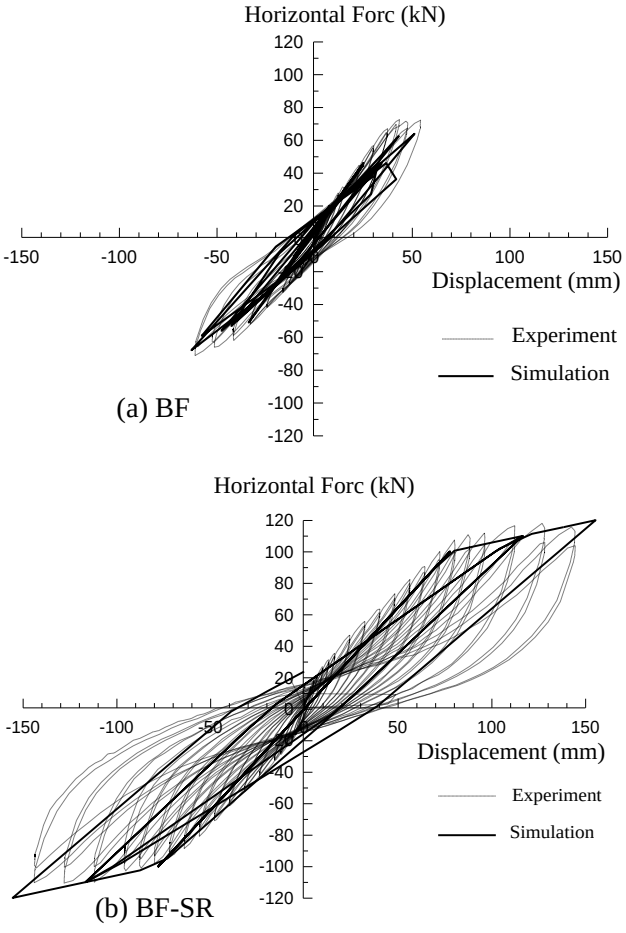

Fig. 15. Simulation and experimental results of bare frame and strengthened bare frame.

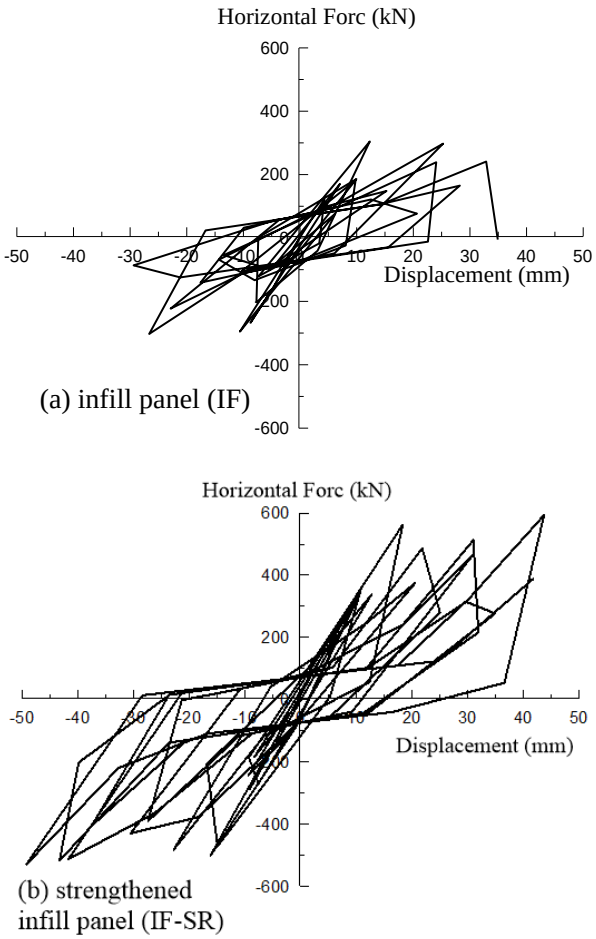

Fig. 16. Simulation of infill panel and strengthened infill panel.

Table 5. Parameters for hysteretic model of IF and IF-SR.

Model parameters	**Infill panel (IF)**	**Strengthened infill panel (IF-SR)**
k_o (kN/mm)	52.60	82.76
V_y (kN)	211.45	384.85
D_y (mm)	4.02	4.65
V_m (kN)	316.28	611.33
D_m (mm)	16.11	14.52
αk_o (kN/mm)	8.67	22.95

Table 6. Strength comparisons between the experiment and the analysis of the specimens IF and IF-SR.

Specimens	IF	IF-SR
Analysis		
Bare frame (kN)	69.34	110.63
Infill panel (kN)	316.28	611.33
Infilled Frame (kN)	385.62	721.96
Experiment		
Infilled Frame (kN)	407	760
Difference (%)	5.25	5.01

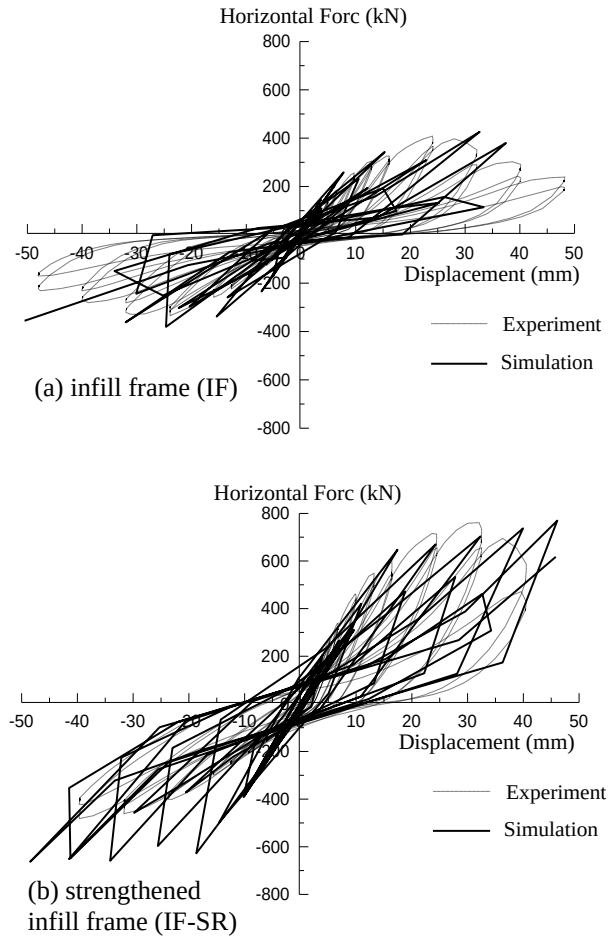

Fig. 17. Experiment and simulation of infilled frame (IF) and strengthened infilled frame (IF-SR).

Acknowledgment

This research is part of the research project "Research and Development for Strengthening of a Prototype School Building for Earthquake Resistant using Expanded Metal and Technology Transferring to a Case Study for School Building in Phan District Chiangrai Community Area", supported by Biodiversity-based Economy Development Office (Public Organization), V & P Expanded Metal, including Chulalongkorn Research Laboratory.

References

[1] P. Lukkunaprasit, A. Ruangrassamee, T. Boonyatee, C. Chintanapakdee, K. Jankaew, N. Thanasisathit, and T. Chandrangsu, "Performance of structures in the MW 6.1 Mae Lao earthquake in Thailand on May 5, 2014 and implications for future construction," *Journal of Earthquake Engineering*, vol. 20, pp. 219-42, 2015.

[2] *Evaluation of Earthquake Damaged Concrete and Masonry Wall Building*, FEMA 306, Federal Emergency Management Agency, Washington D.C., 1998.

[3] M. T. Kazemi and R. Morshed, "Seismic shear strengthening of R/C columns with ferrocement jacket," *Cement and Concrete Composites*, vol. 27, pp. 834-842, 2005.

[4] *Guide for the Design, Construction, and Repair of Ferrocement*, ACI 549.1R-93, ACI Committee, American Concrete Institute, MI, USA, 1993.

[5] Y. A. Al-Salloum "Influence of edge sharpness on the strength of square concrete columns confined with FRP composite laminates," *Composites Part B: Engineering*, vol. 38, pp. 640–50, 2006.

[6] L. Wang, "Effect of corner radius on the performance of CFRP-confined square concrete column," M.Phil. thesis, Department of Building and Construction, City University of Hong Kong, Hong Kong, 2007.

[7] A. B. M. A. Kaish, M. R. Alam, M. Jamil, M. F. M. Zain, and M. A. Wahed, "Improved ferrocement jacketing for restrengthening of square RC short column," *Construction and Building Materials*, vol. 36, pp. 228–237, 2012.

[8] S. Aykac, I. Kalkan, and M. Seydanlioglu, "Strengthening of hollow brick infill walls with perforated steel plates," *Earthquakes Structures*, vol. 6, no. 2, pp. 181–99, 2014.

[9] B. Aykac, E. Ozbek, R. Babayani, M. Baran, and S. Aykac, "Seismic strengthening of infill walls with perforated steel plates," *Engineering Structures*, vol. 152, pp. 168–179, 2017.

[10] A. Leeanansaksiri, P. Panyakapo, and A. Ruangrassme, "Seismic capacity of masonry infilled RC frame strengthening with expanded metal ferrocement," *Engineering Structures*, vol. 159, pp. 110-27, 2018.

[11] S. Aykac, E. Ozbek, I. Kalkan, and B. Aykac, "Discussion on "Seismic capacity of masonry infilled RC frame strengthening with expanded metal ferrocement," *Engineering Structures*, vol. 171, pp. 928-932, 2018.

[12] N. Ismail, T. El-Maaddawy, and N. Khattak, "Quasi-static in-plane testing of FRCM strengthened non-ductile reinforced concrete frames with masonry infills," *Construction and Building Materials*, vol. 186, pp. 1286–1298, 2018.

[13] M. TahamouliRoudsaria, M. Torkamana, A. R. Entezarib, H. Rahimia, and K. Niazi, "Experimental investigation of strengthening reinforced concrete moment resisting frames using partially attached steel infill plate," *Structures*, vol. 19, pp. 173–183, 2019.

[14] A. Saneinejad and B. Hobbs, "Inelastic design of infilled frames," *Journal of Structural Engineering, ASCE,* vol. 6682, pp. 634-50, 1995.

[15] S. Panyamul, P. Panyakapo, and A. Ruangrassamee, "Seismic shear strengthening of reinforced concrete short columns using ferrocement with expanded metal," *Engineering Journal*, vol. 23, no. 6, pp. 175-189, 2019.

[16] *Standard Test Method for Compressive Strength of Hydraulic-Cement Mortars*, ASTM Standard No. ASTM C349, American Society for Testing and Materials (ASTM), 1997.
[17] *Steel Bars for Reinforced Concrete: Round Bars*, TIS 20-2543, Thai Industrial Standard (TIS), Department of Industrial Product Standard, Ministry of Industry, Thailand, 2000.
[18] *Expanded Metal Standard by Japanese Industrial Standard*, JIS Standard No. JIS G3351, Japanese Standards Association, 1987.
[19] P. N. Dung and A. Plumier, "Behavior of expanded metal panels under shear loading," in *Proceedings of SDSS RIO 2010 Stability and Ductility of Steel Structures Janeiro*, 2010, pp. 1101-1108.
[20] *Standard Test Method for Compressive Strength of Masonry Prisms*, ASTM Standard No. ASTM C1314, American Society for Testing and Materials (ASTM), 2007.
[21] *Standard Test Method for Diagonal Tension (Shear) in Masonry Assemblages*, ASTM Standard No. ASTM E519, American Society for Testing and Materials (ASTM), 2002.
[22] *Standard for Reinforced Concrete Building: Working Stress Design Method*, EIT 1007-34, The Engineering Institute of Thailand, Bangkok, Thailand, 1991.
[23] Federal Emergency Management Agency, "Interim testing protocol for determining the seismic performance characteristics of structural and nonstructural components," Redwood City, Report no. FEMA 461, 2007.
[24] P. Panyakapo, "Cyclic pushover analysis procedure to estimate seismic demands for buildings," *Engineering Structures*, vol. 66, pp. 10-23, 2014.
[25] A. J. Carr. "RUAUMOKO computer program," University of Canterbury, Christchurch, New Zealand, 2006.
[26] M. Saiidi and M. A. Sozen, "Simple and complex models for nonlinear seismic response of reinforced concrete structures," Department of Civil Engineering, University of Illinois, Urbana, Illinois, Report UILU – ENG-79-2031, Aug. 1979.
[27] W. G. Stewart, "The seismic design of plywood sheathed shear walls," Ph.D. thesis, Department of Civil Engineering, University of Canterbury, 1987.

Suvawat Longthong received the B.Eng. degree in civil engineering from Sripatum University, Bangkok, Thailand in 1999. He has worked in the construction industry as a civil engineer since 1999. His experience involves the construction of buildings and hydropower dams. Since 2014, he has been a student in Master of Engineering Program in Civil Engineering, Sripatum University. His research interests include building design and seismic retrofit of buildings.

Phaiboon Panyakapo received the B.Eng. degree in civil engineering from Kasertsart University, Bangkok, Thailand in 1982 and the M.Eng. and D.Eng. degrees in structural engineering from Asian Institute of Technology, Pathumthani, Thailand, in 1984 and 1999. From 1997-2000, he was a lecturer at Department of Civil Engineering, School of Engineering, Sripatum University. Since 2004, he has been an Associate Professor at the Civil Engineering Department, Sripatum University, Bangkok, Thailand. He is the author of three books, more than 20 articles, and 1 invention (in patent process). His research interests include building design, seismic design, precasted concrete design, performance based design and seismic retrofit of buildings. He is an Associate Editor of the journal, Sripatum Review of Science and Technology.

Anat Ruangrassamee received the B.Eng. degree in civil engineering from Chulalongkorn University, Bangkok, Thailand in 1996 and the M.Eng. and Ph.D. degrees in civil engineering from Tokyo Institute of Technology, Japan, in 1998 and 2001. He has worked at Department of Civil Engineering, Faculty of Engineering, Chulalongkorn University since 1996. Currently, he is an Associate Professor at the Civil Engineering Department, Chulalongkorn University, Bangkok, Thailand. His research interests include earthquake engineering and seismic retrofit of structures.